한국동력기계공학학회지 제6권 제4호 pp.73~80 2002년 11월

Controller Design and Experiment to Levitate a Rotor in an Active Magnetic Bearing System
능동 자기 베어링 시스템의 제어기 설계 및 연구

Yu Chang, Sung-Hyo Shim, Joo-Ho Yang
창유 · 심성효 · 양주호

Key Words : Rigid(강성), Rotor Bearing System(로터 베어링 시스템), Digital Signal Processor (디지털 신호 처리기), PD control(PD 제어), Coupling Effect(간섭 효과), Active Magnetic Bearing(능동 베어링 시스템)

요약 : 이 논문은 MIMO 능동 자기 베어링 시스템에 있어서의 병진 및 회전(기울기)운동을 하는 횡축형 강체 로터의 동적 거동을 모델링하고, 로터 양 끝단의 간섭효과를 고려한 제어방법을 제안한다. 제어기는 DSP 보드를 이용하였으며, 설계된 제어기의 타당성을 시뮬레이션 및 실험을 통하여 검증하였다.

Notation

A_r : rigid body system matrix
B_r : rigid body input matrix
C_r : rigid body output matrix
C_l : current amplifier capacitance [C]
F_l, F_r : force of left and right bearing
$G(s)$: transfer function of plant
$G_{11}, G_{12}, G_{21}, G_{22}$: transfer function of electromagnets
I_0 : the mass moment of inertia of the shaft for x-axis or y-axis
$i_{c_{l,r}}$: control current on left and right electro-magnets
$K_1(s)$: transfer matrix of the displacement controller
$K_2(s)$: transfer matrix of the slope controller
K_{dx} : displacement speed gain
K_{dt} : slope speed gain
K_p : proportional parameter
K_{px} : displacement parameter
K_{pt} : slope parameter
L : electromagnets coil inductance [H]
l_1 : the distance from the rotor mass center to the bearing [m]
l_3 : the distance from the rotor mass center to the sensor [m]
m : rotor mass [kg]
R_l : current amplifier resistance [Ω]
R_l : electromagnets coil resistance [Ω]
r : external disturbance signal
T_d : differential parameter
u : control input vector
u_1, u_2 : control input vectors on left and right side [V]
u_x : control input vectors of displacement [V]
u_t : control input vectors of slop [V]
$V_{c_{l,r}}$: control outputs on left and right side of controller [V]
$V_{s_{l,r}}$: control outputs on left and right side of sensor [V]
x_r : state vector of rigid rotor

Manuscript received: July 11, 2002
Yu Chang, Sung-Hyo Shim: Graduate School, Pukyong National University(PKNU)
Joo-Ho Yang: School of Mechanical Engineering, PKNU

x_0 : the horizontal displacement at the mass center of the rotor [m]

x_{br}, x_{bl} : the horizontal displacement at the points of left and right bearing [m]

x_{xr}, x_{xl} : the horizontal displacement at the points of left and right sensor [m]

y_r : output vector of the rigid rotor

y_1, y_2 : output vector on left and right side

α : current amplifier. electromagnets coil gain

β_1 : coefficient of displacement/voltage relation in sensor [V/m]

λ : the control voltage proportional to the other side

θ : slope angular to the axis in county clockwise [1/s]

$k1, k_2$: displacement-force coefficient and current-force coefficient of bearing

1. Introduction

Active magnetic bearing (AMB) is a kind of novel high performance bearing for its advantages associated with AMB technology as the following aspects. Firstly, advantages of the AMB include no wear and no lubrication requirements. Therefore, the AMB is an environmentally friendly technology that results in the reduction of equipment maintenance and waste associated with the replacement of used lubricants and bearings.

Another major advantage of AMB system is that they are capable of operating under much higher speeds than conventional rolling element bearings with relatively low power losses. AMB system also have active vibration control capabilities.

On the other hand, majorities of AMB machines installed analog controller which has some drawbacks such as the noise may lead to the inaccurate results and when the controller gets heater it may change the system parameters. Fortunately, such rapid development of micro- processor as DSP makes it feasible to implement the design approximately approaching continuous system. Moreover, it compensates the disadvantages of analog controller and has the flexibility to design as digital controller.

In this MIMO AMB rigid rotor system, we assume the rotor is a simple mechanical system, dose not bend but rather experiences only translational or slop motion as a rigid body.

Furthermore, the horizontal rotor is levitated by electromagnets at each end of the rotor. Sensors, outside of the electromagnets, measure displacement at both ends of the rotor. It is hard to ensure the satisfied control performance, if control the rotor at each end independently, because the coupling effect from one end of the rotor lead to a slight amount at the other. So that a controller is demanded to consider this effect to the displacement on its left and right side.

In order to improve the rotor recovery performance to equilibratory point, a suggested control method was introduced compensating rotor slope motion to its principal axis. Then, a digital PD controller was designed and executed on a DSP board. Last, an evaluation to this control system was come up with by comparison the simulation results to the experiment results.

2. Rigid AMB System Modeling

In the AMB system as shown in Fig. 1, the rotor as shown in Fig. 3 is assumed as a rigid body. In the Current ample and magnetic coil circuit as shown in Fig. 2, we considered the DC gain is 1 form point c to point b, and ignored the effect of the inductance, then the overall statespace equation becomes to equation (1)

Fig. 1 Schematic diagram of magmetic bearing control system

Fig. 2 Current amplifier and electromagnetic coil

Fig. 3 Rigid body motion of rotor

$$\dot{x}_r = \begin{bmatrix} 0 & 1 & 0 & 0 \\ \alpha_1 & 0 & 0 & 0 \\ 0 & 0 & 0 & 1 \\ 0 & 0 & \alpha_2 & 0 \end{bmatrix} \begin{bmatrix} x_0 \\ \dot{x}_0 \\ \theta \\ \dot{\theta} \end{bmatrix} + \begin{bmatrix} 0 & 0 \\ \alpha b_1 & \alpha b_1 \\ 0 & 0 \\ -\alpha b_2 & \alpha b_2 \end{bmatrix} \begin{bmatrix} V_{C_l} \\ V_{C_r} \end{bmatrix} \quad (1)$$

where, $\alpha_1 = \alpha \frac{k_2}{m}$, $\alpha_2 = 2\frac{k_2}{I_0} l_1^2$, $\alpha b_1 = \alpha \frac{k_2}{m}$, and $\alpha b_2 = \alpha \frac{k_2}{I_0} l_1$. The parameters of k_1 and k_2 are the displacement-force coefficient and current-force coefficient of bearing, I_0 is the mass moment of inertia of the shaft for x-axis or y-axis, ignore the inductance effect of magnetic coil, then we obtain $\alpha = \frac{1}{R_L}$.

Output equation is given by equation (2)

$$y_r = \begin{bmatrix} V_{s_l} \\ V_{s_r} \end{bmatrix} = \begin{bmatrix} c_1 & 0 & -c_2 & 0 \\ c_1 & 0 & c_2 & 0 \end{bmatrix} x_r \quad (2)$$

where, $c_1 = \beta_1$, $c_2 = \beta_1 l_3$, the β_1 is linear displacement/voltage parameter of sensor.

Fig. 4 Block diagram, of the AMB system

From the State space equation above, overall transfer function matrix is obtained as shown by equation (3). The overall block diagram is Fig. 4.

$$G(s) = C(sI - A)^{-1}B = \begin{bmatrix} G_{11} & G_{12} \\ G_{21} & G_{22} \end{bmatrix} \quad (3)$$

where,

$$G_{11} = \frac{(\beta_1 \alpha c_1 + \beta_2 \alpha c_2)s^2 - (\beta_1 \alpha c_1 \alpha_2 + \beta_2 \alpha c_2 \alpha_1)}{s^4 - (\alpha_1 + \alpha_2)s^2 - \alpha_1 \alpha_2}$$

$$G_{12} = \frac{(\beta_1 \alpha c_1 + \beta_2 \alpha c_2)s^2 - (\beta_1 \alpha c_1 \alpha_2 - \beta_2 \alpha c_2 \alpha_1)}{s^4 - (\alpha_1 + \alpha_2)s^2 - \alpha_1 \alpha_2}$$

$G_{22} = G_{11}$, $G_{21} = G_{12}$

Through the dynamic experiment of the MB system and the numerical analysis, the parameters of systems are as following $\alpha_1 = 58881$, $\alpha_2 = 107588$, $\alpha\beta_1 = 6.584$, $\alpha\beta_2 = 114.176$, $c_1 = 10000$, $c_2 = 1308$ and

nominal transfer functions are

$$G_{11}=G_{22}=\frac{215186.142s^2-15877445495.9119}{s^4-166469.0361s^2+6334879910.6609}$$

$$G_{12}=G_{21}=\frac{-83497.1788s^2-1709258184.5393}{s^4-166469.0361s^2+6334879910.6609}$$

The frequency response is as shown in Fig. 5.

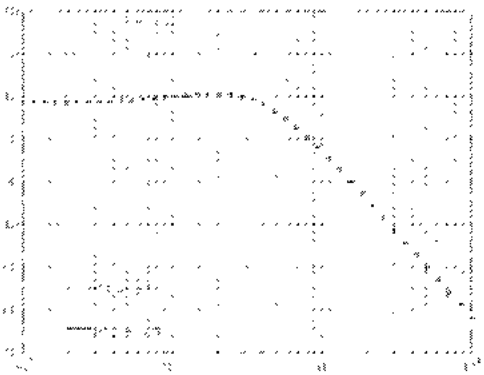

Fig. 5 Frequency response of the AMB

3. Controller Design

Basing on the results of state space equation of the system, a controller is designed to stabilize the levitation for the rigid rotor.

The rotor motion is under the coupling effect from the two sides displacement , without this consideration of the coupling effect, it is hard to get the satisfied control performance. Therefore, in this part, introduce a method as shown in Fig. 3.1 using the negative feedback of the other side signal to compensate the slope displacement caused by the slop movement, as well as improving recovery ability to the equilibratory point of displacement. That is to say, the controller derives a displacement signal from one side to the other side as the shown in equation (4) and (5).

$$K_1(s)=K_p(1+T_dS) \tag{4}$$

$$K_2(s)=\lambda K_1(s) \tag{5}$$

The block diagram of the suggested controller is shown in Fig. 6.

Fig. 6 Block diagram of the suggested controller

In this study, $K_1(s)$ as shown in equation (4) is PD controller on the left and right sides. Slope displacement is controlled by controller $K_2(s)$ as shown in equation (5). λ is the control voltage proportional to the other side.

On principle of the suggested control method in this paper, compute equation (1) into the form of equation (6) and (7).

$$m\ddot{x}_0=k_{mx}x_0+k_2aV_{C_l}+k_2aV_{C_r} \tag{6}$$

$$I_0\ddot{q}=k_{mt}q-k_2l_1aV_{C_l}+k_2L_1aV_{C_r} \tag{7}$$

where, $k_{mk}=2k_1$ and $k_{mt}=2k_1l_1^2$.

We defined u_x and u_t as following.

$$u_x\equiv k_2aV_{C_l}+k_2aV_{C_r} \tag{8}$$

$$u_t\equiv -k_2l_1aV_{C_l}+k_2l_1aV_{C_r} \tag{9}$$

Deriving from equation (6), (7), (8) and (9), we can obtain equation (10) and (11) by which, u_x is the function of x_0 and u_t is the function of θ are shown.

$$m\ddot{x}_0-k_{mx}x_0=u_x \tag{10}$$

$$I_0\ddot{\Theta}-k_{mt}\Theta=u_t \tag{11}$$

And equation (8) and (9) can develop equation (12) and (13) showing that V_{C_l} and V_{C_r} are the function of u_x and u_t.

$$V_{C_l}=\frac{1}{2k_2a}u_x+\frac{1}{2k_2l_2a}u_t \tag{12}$$

$$V_{C_r}=\frac{1}{2k_2a}u_x-\frac{1}{2k_2l_2a}u_t \tag{13}$$

Equation (14) and (15) can be obtained showing the relations between V_{C_l} V_{C_r} and x_0, θ, by substituting equation(10) and (11) into equation (12) and (13).

$$V_{C_l} = \frac{1}{2k_2a}(m\ddot{x}_0 - k_{mx}x_0) + \frac{1}{2k_2l_2a}(I_0\ddot{\Theta} - k_{mt}\Theta) \quad (14)$$

$$V_{C_r} = \frac{1}{2k_2a}(m\ddot{x}_0 - k_{mx}x_0) - \frac{1}{2k_2l_2a}(I_0\ddot{\Theta} - k_{mt}\Theta) \quad (15)$$

As control input, u_x and u_t can be denoted as shown by equation (16) and (17) according to the state feedback control law.

$$u_x = -K_{px}x_0 - K_{dx}\dot{x}_0 \quad (16)$$

$$u_x = -K_{px}\Theta - K_{dt}\dot{\Theta} \quad (17)$$

Then combining with equation (10), (11), (16), and (17), gives equation(18) and (19) as follow.

$$\ddot{x} = \frac{k_{mx}}{m}x_0 - \frac{K_{px}}{m}x_0 - \frac{K_{dx}}{m}\dot{x}_0 \quad (18)$$

$$\ddot{\Theta} = \frac{k_{mx}}{I_0}\Theta - \frac{K_{px}}{I_0}\Theta - \frac{K_{dx}}{I_0}\dot{\Theta} \quad (19)$$

where,

$$K_{px} = 2k_1\alpha\beta_1(1+\lambda)K_p \quad (20)$$

$$K_{dx} = 2k_1\alpha\beta_1(1+\lambda)K_pT_d \quad (21)$$

$$K_{pt} = 2k_1\alpha\beta_1(1-\lambda)K_p \quad (22)$$

$$K_{dt} = 2k_1\alpha\beta_1(1-\lambda)K_pTd \quad (23)$$

The AMB system block diagram becomes as shown in Fig. 7.

Fig. 7 Block diagram of PD control system

Using Laplace transformation, we obtain the characteristics equation as shown by equation (24) for this closed loop system.

According to Routh-Hurwitz stable criterion for equation (24), we can compute the stable condition as shown in equation (25) and (26).

$$(ms^2 + K_{ds} + K_{px} - k_{mk})(I_0s^2 + K_{dt}s + K_{pt} - k_{mt}) = 0 \quad (24)$$

$$K_{dx}(K_{px} - k_{mx}) > 0 \quad (25)$$

$$K_{dt}(K_{pt} - k_{mt}) > 0 \quad (26)$$

In the controlled system with this suggested controller, the transfer function of each part of this system and the controllers are denoted as shown by equation (27), (28) and (29), similarly, the equation (30) and (31) denote the closed loop transfer function from R_1 to Y_1 and form R_2 to Y_1.

$$G_{21}(s) = \frac{N_{G_{21}}(s)}{D_{G_{21}}(s)}, \quad G_{22}(s) = \frac{N_{G_{22}}(s)}{D_{G_{22}}(s)} \quad (27)$$

$$G_{11}(s) = \frac{N_{G_{11}}(s)}{D_{G_{11}}(s)}, \quad G_{12}(s) = \frac{N_{G_{12}}(s)}{D_{G_{12}}(s)} \quad (28)$$

$$K_1(s) = \frac{N_{K_1}(s)}{D_{K_1}(s)}, \quad K_2(s) = \frac{N_{K_2}(s)}{D_{K_2}(s)} \quad (29)$$

$$\frac{Y_1(s)}{R_1(s)} = \frac{D_{kl}(s)\,(N_{G_{11}}(s)N_A(s) - N_B(s)N_{G_{21}}(s))}{N_A(s)N_A(s) - N_B(s)N_B(s)} \quad (30)$$

$$\frac{Y_1(s)}{R_2(s)} = \frac{D_{kl}(s)\,(N_{G_{12}}(s)N_A(s) - N_B(s)N_{G_{22}}(s))}{N_A(s)N_A(s) - N_B(s)N_B(s)} \quad (31)$$

where,

$$N_A(s) = D_{kl}(s)D_{G_{12}}(s) + N_{G_{11}}(s)N_{k_1}(s) + N_{G_{12}}(s)N_{k_2}(s) \quad (32)$$

$$N_B(s) = -N_{G_{11}}(s)N_{k_2}(s) + N_{G_{12}}(s)N_{k_2}(s) \quad (33)$$

By using the left and right displacement at points of the bearings x_{bl}, x_{br} as control input, equation (16) and (17) can be written into the form of equation (34) and (35).

$$u_{xl}(s) = -K_p(1+T_ds)x_{bl}(s) - \lambda K_p(1+T_ds)x_{br}(s) \quad (34)$$

$$u_{xr}(s) = \begin{matrix} -K_p(1+T_d s)x_{br}(s) \\ -\lambda K_p(1+T_d s)x_{bl}(s) \end{matrix} \quad (35)$$

The roots of the characteristics equation of equation (24) were expected at the positions where can let the system is of satisfied settling time and the maximum overshot critical limit. Such parameters of PD controller as K_p, λ and $T_d$were tuned and final amount was selected as $K_p = 1.2,\ \lambda = 0.4,\ T_d = 0.0002$.

The frequency responses of closed loop system is shown in Fig. 8.

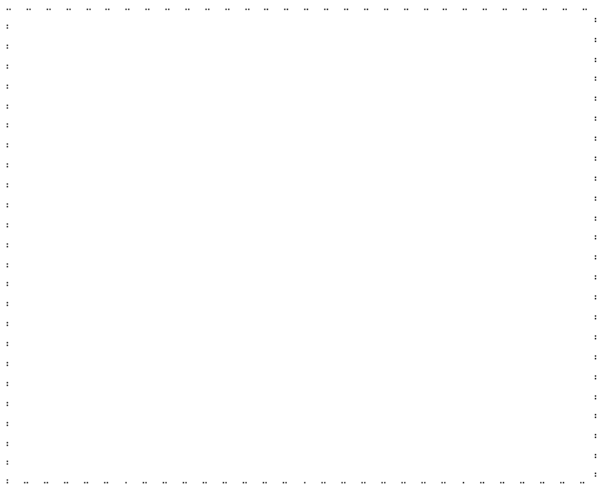

Fig. 8 Frequency responses of closed loop system

4. Simulation and Experiment Results

Fig. 9 is the time response for the impulse disturbance in the case of local control method by using analog lead compensator designed by a manufacture company. While Fig. 10 is the time response for the impulse disturbance in the case of suggested control method by using external digital PD controller. And Fig. 11 is the simulation result for the time responses of the impulse disturbance.

From the comparison of the results in Fig. 9 and Fig. 10, we can observe clearly that, firstly, the settling time is more quickly in Fig. 10, secondly, the stead state error in the later case is much smaller than the form.

From the comparison of the results in Fig. 9 and 10, wecan observe clearly that, firstly, the settling time is more quickly in Fig. 10, secondly, the stead state error in the later case is much smaller than the former. In other worlds, this suggested method improved the performance dramatically than the local control method. By comparison Fig. 10 to Fig. 11 we satisfy that the simulation results and the experiment results are very uniform, which is identified that the simulation according to the suggested method is correct.

Fig. 12 shows the response performance for the step disturbance in the case of local control method by using analog lead compensator. And Fig. 13 is the response performance for the step disturbance in the case of suggested control method by using external digital PD controller. While Fig. 14 is the simulation result for the time responses of the impulse disturbance.

Similarly, the comparison of the results in Fig. 12 and Fig. 13, shows that the overshot is smaller for step disturbance in Fig. 13. That isto say, this suggested method improved the performance. Also, the uniform results of simulation and experiment as shown in Fig. 13 and Fig. 14, identified that the simulation according to the suggested method is correct again.

Besides, even under the situation of the AMB system being overturned in 360 degree along rotor axis direction or lateral direction,

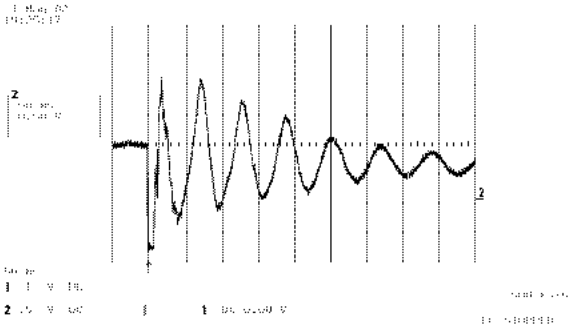

Fig. 9 Time response for the impulse dist-urbance in the case of local control method by useing analog lead con-pensator

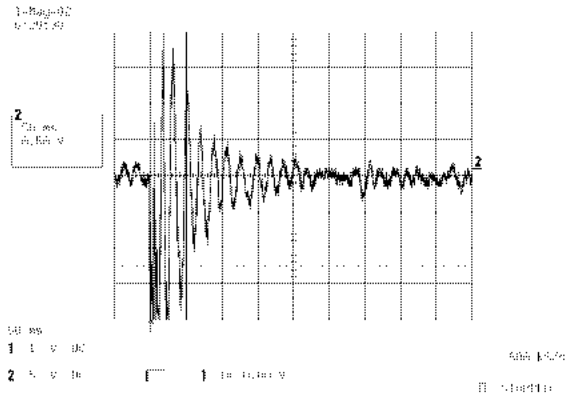

Fig. 10 Time response for the impulse disturbance in the case of suggested control method by useing external digital PD controller

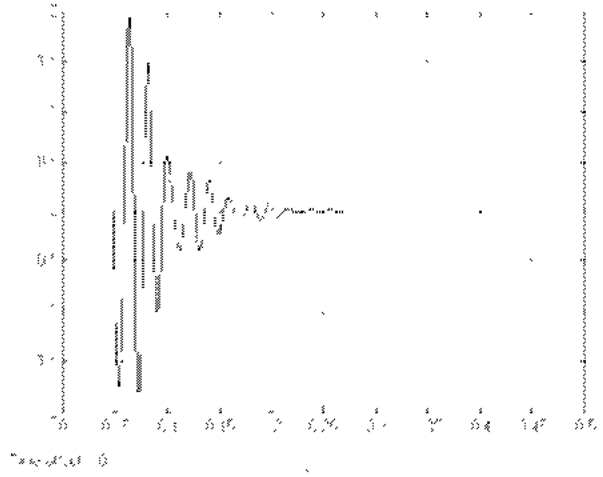

Fig. 11 Simulation for the time response of impulse disturbance

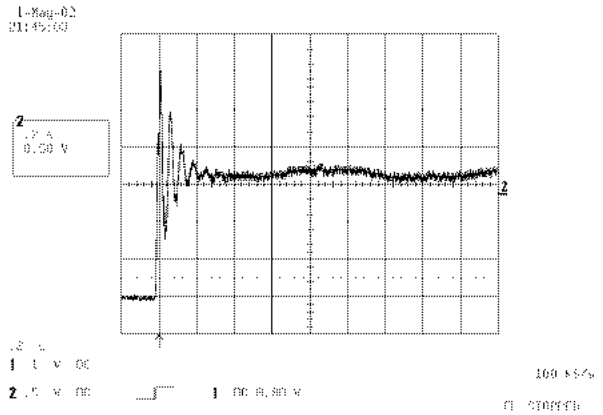

Fig. 12 The response for the step disturbance in the case of local control method by useing analog lead compensator

good performance of the AMB system is afforded by this controller.

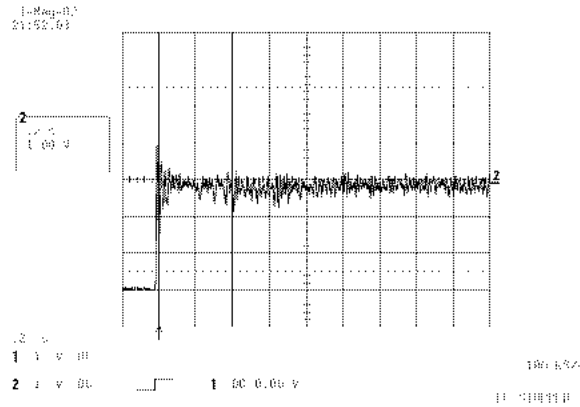

Fig. 13 Time response for the step disturbance in the case of suggested control method by useing external digital PD controller

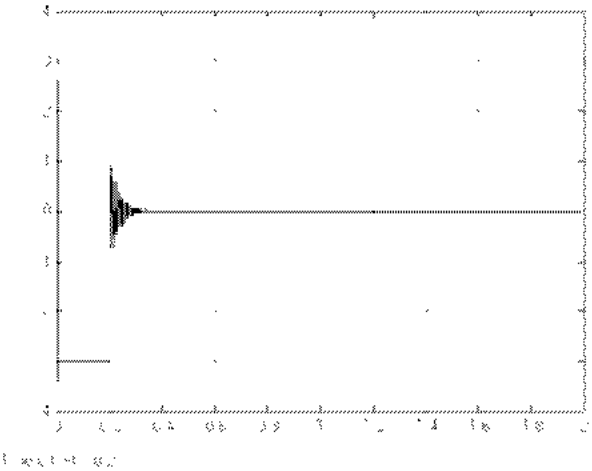

Fig. 14 Simulation for the time response of step disturbance

5. Conclusion

In this study, a suggested control method is presented. This method is to derivate a sensors output signal of the rotor slop form one side to the other side as feedback signal. It can be certified that this method improved the settling , stability and recovery ability form results in terms of the comparison of experiment results to simulation for the time responses of both impulse disturbance and step disturbance and the comparison of experiment results to simulation for the recovery performance.

The simulations and experiments were in

good agreement and showed the method's efficiency and robustness as well as the pertinence of the technological choices made.

Acknowledgement

This work was partially supported by the Brain Korea 21 project in 2002.

References

1. S. H. Shim, M. S. Choi, C. H. Kim and et al., "A Study on Modeling for the Magnetic Bearing System by Numerical Analysis", The Korean Society for Power System Engineering, Vol. 5, No. 4, pp. 53~60, 2001
2. S. H. Shim, C. H. Kim, J. H. Yang, "A Study on Modeling and Identification for the Magnetic Bearing System", The Korean Society for Power System Engineering, Vol. 5, No. 4, pp. 44~52, 2001
3. D. H. Moon, "Vibration Analysis for Frame Structures Using Transfer of Dynamic Stiffness Coefficient", Journal of Sound & Vibration, Vol. 234, No. 5, pp. 725~736, 2000
4. M. Hirschmanner, N. Steinschaden, H. Springer, "Adaptive Control of a Rotor Excited by Destabilizing Cross-coupling Forces", IFToMM Sixth International Conference on Rotor Dynamics Proceedings, ISBN 0 7334 1962 3, pp. 38~46, 2002
5. H. J. Ahn, I. H. Park, D. C. Han, "A Novel Frequency Domain Identification of a MIMO AMB Rigid Rotor System", IFToMM Sixth International Conference on Rotor Dynamics Proceedings, ISBN 0 7334 1962 3, pp. 93~101, 2002